

USING SMOOTHED PARTICLE HYDRODYNAMICS TO STUDY WAVE IMPACT ON FLOATING OFFSHORE PLATFORMS: THE EFFECT OF MOORING SYSTEM

Murray RUDMAN* and Paul W CLEARY

¹ CSIRO Mathematical and Information Science, Clayton, Victoria 3169, AUSTRALIA

*Corresponding author, E-mail address: Murray.Rudman@csiro.au

ABSTRACT

The highly non-linear impact of a rogue wave on a floating, moored offshore structure is a problem that has significant practical application in the safety of offshore oil and gas production. It is a difficult problem to simulate with standard CFD techniques and in this paper we apply the Smoothed Particle Hydrodynamics (SPH) technique to rogue wave impact on a semi-submersible platform. The simulation results show that the scenario can be successfully simulated, and indicate that the effect of wave impact angle plays a minor role in most of the kinematics of platform motion. More importantly, it is shown that the tension in the mooring cables, and their propensity to break, depends strongly on the wave impact angle. The nature of the mooring system plays a significant role in the kinematics of platform motion and the cable loading, as do the material properties of the cables. SPH is seen to be a useful tool in the design of floating offshore platforms and mooring systems.

INTRODUCTION

For the interaction of small amplitude waves with geometrically simple structures, good prediction of the wave-structure coupling can be obtained using mathematical approaches that approximate the interaction and dynamics, (Faltinsen 1990, Jain 1997). As the structures become more complex, the prediction becomes more difficult and numerical analysis using techniques such as boundary integral methods becomes necessary (e.g. Nielsen 2003). For irregular, and especially, non-linear large amplitude waves, good prediction becomes increasingly difficult. Wave-structure interaction in such cases involves many interacting physical phenomena, the most important being severe free surface deformation and large structural motions. When a structure has additional constraints such as mooring lines and chains, these must also be included in the analysis. Typically, wave tank testing is used to predict these kinds of interactions, however such testing is time consuming and expensive. Computational methods that can perform analyses in the early stages of design are desirable and can reduce the number of design alternatives that require wave tank testing. Fully three-dimensional Computational Fluid Dynamics (CFD) simulation of the interaction therefore becomes an attractive alternative for obtaining understanding of the essential mechanics of the interaction and consequently assisting with design. These kinds of CFD simulations have appeared (e.g. Bunnick and

Buchner 2004, Kleefsman *et al.* 2005, Gomez-Gesteira 2005, Rudman *et al.* 2008 and Cleary and Rudman 2009) although there is still work to be done before they become a commonly used design tool.

A highly non-linear problem that cannot be investigated with analytic or simplified numerical techniques is the impact of 'rogue' waves on offshore structures. In order to simulate rogue wave impact, the CFD technique must be capable of handling very high free surface deformation as well as significant motion of the structure in a simple and robust manner. In this paper we use the Smoothed Particle Hydrodynamics (SPH) technique (Monaghan 1994, Cleary and Prakash 2004). As discussed in Rudman *et al.* 2007, SPH has a number of natural advantages over the Volume-of-Fluid (VOF) technique often used for such cases (e.g. Bunnick and Buchner 2004 and Kleefsman *et al.* 2005).

The aim of this paper is to understand how the mooring systems can be modified to best withstand rogue wave impacts and in so doing, illustrate the utility of SPH to the fully-coupled problem of wave impact on a moored offshore platform. The method allows prediction of the platform motion and provides estimates of the tensions in the mooring cables. Four different mooring systems are considered for wave impact angles from normal impact (0°) to 45°. This paper extends the work of Rudman *et al.* (2008, 2009) and Cleary and Rudman (2009) by considering two new mooring systems that are a hybrid of those considered previously. The results show a clear distinction in platform behaviour between different mooring systems, illustrating the potential of SPH for use in the design of platforms and mooring systems.

SIMULATION METHOD AND CONFIGURATION

SPH is a computational method that has been widely applied to industrial and environmental flows (e.g. Cleary 1998, Cleary and Prakash 2004). It has more recently been applied to oceanic and offshore hydrodynamics (see for example Gomez-Gesteira 2005, Shao 2006, Rudman *et al.* 2007, Cleary and Rudman 2009).

Unlike most numerical techniques for CFD, SPH does not utilize a fixed nodal grid. Instead, the discretised equations of motion are solved on a set of moving "particles". Each particle carries mass, momentum and energy and moves with the local fluid velocity. There is no explicit connectivity of the particles which means, for example, that particles that are close neighbours at one instant in time can be quite distant from each other at a

later time. A detailed description of the method can be found in Monaghan (1992, 1994), Cleary (1998) and Cleary and Prakash (2004).

Structure Representation

Arbitrary boundaries and structures are easily handled in our implementation of SPH. The surface of the floating platform is discretised with a distinct set of boundary particles whose positions are fixed relative to each other. The boundary particles repel fluid particles that approach them with a normal force (Monaghan 1994).

Forces on the structure are determined by integrating the point-wise local forces applied by the fluid to each of the particles representing the structure. The net torque on the structure is likewise calculated by summing the local torque created by the fluid force at each particle location in the structure. These net forces and torques used in Newton's equations of motion for the structure.

Other information required for the structure are its mass, centre of mass and the moments of inertia about the three axes passing through the centre of mass. The mass is set and the others estimated from assumed distribution of steelwork and pontoon ballast.

The natural coupling between the fluid flow and the solid structure motion in the SPH method automatically accounts for the lift, drag and added mass of the interaction because they are based on the detailed spatial distribution of surface forces at all points of the structure. In six-degrees of freedom type models, these quantities need to be explicitly specified using assumed lift, drag and added mass coefficients.

Domain setup

Details of the semi-submersible platform considered in this study are presented schematically in Figure 1. The global computational domain is shown schematically in Figure 2 and the mooring systems in Figure 3.

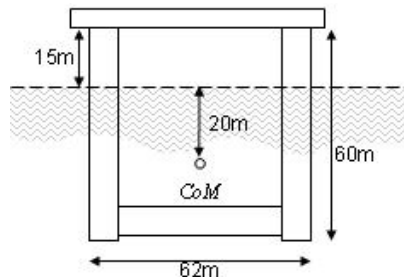


Figure 1: Schematic of the semi-submersible platform.

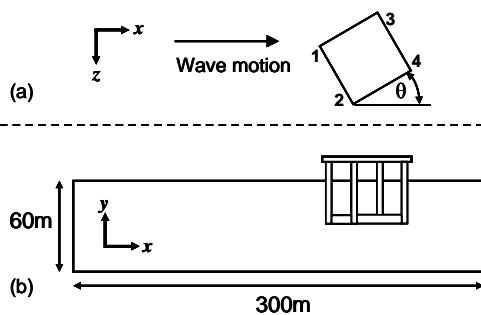


Figure 2: Computational domain. (a) plan view (x - z plane) showing orientation with respect to the wave motion (θ) and 1-4 denote mooring cable ID. (b) elevation view (x - y plane). Domain size is $x=300$ m, $z=150$ m.

With reference to Figure 2a, the wave impact angles considered in this paper are 0, 15, 30 and 45°. The computational domain is periodic in both horizontal (x and z) directions. It is 300 m in the direction of wave motion and 150 m in the transverse direction. The depth of water subject to fluid motion is set to 60 m although the platform is assumed to be sitting in 500 m of water. The cables extend to this full depth. The boundary condition on the bottom of the 60 m fluid layer are free-slip. This approximation is currently required in order to limit the total number of SPH particles in the calculation to a manageable number. Around 1 million fluid particles with a spacing of 1.5 m are used to represent the water. The structure is represented by approximately 200,000 particles with an average particle spacing of 0.5 m. Each simulation takes approximately 300 hours on a single CPU 3 GHz Pentium for 80 s of simulation.

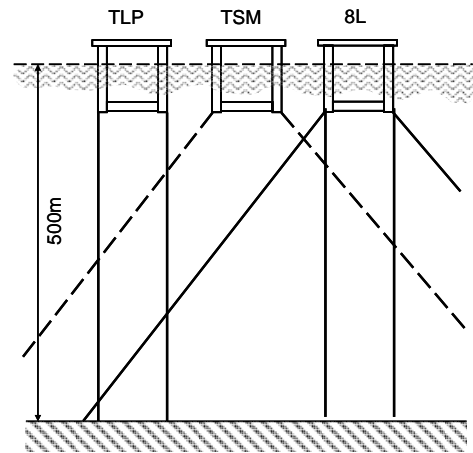


Figure 3: Schematic of the mooring systems. Left is the Tension Leg (TLP) system, centre is the Taut Spread Mooring system (TSM) and right is a combination of both (or "8L", 8 lines system). The diagonal cables make an angle of 45 degrees with the ocean floor.

The total weight of the structure is set to 34,600 tonnes. The centre of mass lies under the centre of the platform, 20 m below the water surface. The draft of the platform is 45 m (see Figure 1) with a 15 m nominal clearance of its underside from the ocean surface.

In practice, multiple cables and/or chains are used to moor each corner of the platform to the ocean floor. To simplify the problem analysis in this study, for the TLP and TSM mooring systems, each column of the platform is connected to the ocean floor with a single composite cable, each of which represents three 150 mm steel cables with an assumed Young's modulus of 1.5×10^{11} (Raouf and Kraincanic 1995). This is not a limitation of the method and multiple cables with different attachment points could be used. For the "8L" systems, each column is connected to the ocean floor with two cables: one vertical and one diagonal. Two different 8L systems are considered. In the first, all cables are steel, each with the same properties as the TLP/TSM systems. This is referred to the 8LS (8-line steel) system. In the second 8L system, the vertical cables are steel and the diagonal cables are polyester with a very different strength and elastic behaviour. This is referred to as the 8LPS (8-Line Polyester and Steel) system.

For all configurations, the self-weight of the cables is ignored as are any drag effects on the cables due to fluid motion. These are expected to be very small compared to

the forces due to wave impact on the platform. In tension, each steel cable is modelled as a linear spring. When the cable extension is less than zero (i.e. the cable is slack) there is zero tension. In the case of the vertical steel cables (for TLP and both 8LS systems), the equivalent spring stiffness is $1.7 \times 10^7 \text{ N m}^{-1}$. For the diagonal steel cables (TSM and 8LS systems) it is $1.13 \times 10^7 \text{ N m}^{-1}$ due to the longer cable length. For the diagonal cables in the 8LPS, a non-linear spring was assumed based on experimental studies of polyester rope reported in Petruska *et al.* (2005). Values for a 270 mm diameter polyester rope were modelled which suggests a non-linear spring in which the tension T as a function of cable extension δL is

$$T = \frac{20F_B \delta L}{L_0 - 29\delta L}, \quad (1)$$

where L_0 is the unloaded cable length and F_B is the maximum breaking load the cable can support ($1.9 \times 10^7 \text{ N}$). As with the steel cables, we assume that the single computational cable represents three real polyester cables, each with these properties.

For the TLP and both 8LS configurations, the total initial tension in the vertical cables is set to 1000 tonne weight, with each of the 4 vertical cables initially supporting one quarter of this. For the TSM configuration and diagonal cables in the 8L systems, the cables are initially tight, but have no tension.

Wave generation

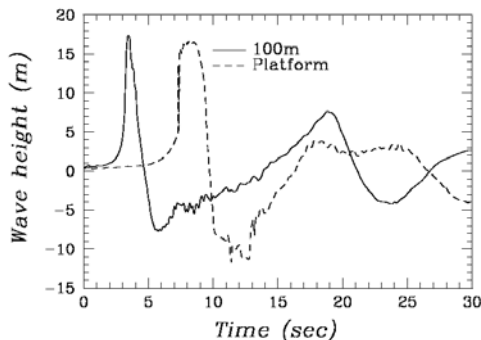


Figure 4: Water height profile: Solid line is 100 m prior to impact with the platform and dashed line is the initial location of the centre of mass of the platform.

The rogue wave used in all simulations here is generated using a wave-maker driven by a localised momentum source away from the platform. The momentum source operates for a short time at the start of the simulation and is then switched off well before wave impact. By adjusting the wave maker control parameters we create a wave with the desired characteristics (height, speed, shape) and allow it to travel towards the platform. For the wave considered here, the height is 17 m above the nominal free surface with a following trough of approximately 8 m (see Figure 4). The peak of this wave is just sufficient to hit on the underside of the platform deck if there were no platform motion. The speed of this wave is approximately 20 m/s on impact which occurs at 6 s.

Platform degrees of freedom

The platform is free to move as a result of a combination of wave impact and restoring (cable) forces. We use

standard nomenclature of Surge, Heave and Sway for global (x,y,z) motions. The surge (x) direction is specified by the wave's direction of motion at impact. In practical terms, the angle the deck makes with the horizontal is the most important angular measure because it correlates with danger to people on the platform deck. To define an appropriate angle, we define the pitch (θ_p) as the angle between the global coordinate y -axis, \mathbf{j} , and the platform deck normal (\mathbf{n}_D) expressed in global coordinates, regardless of the direction in which \mathbf{n}_D points. This definition of pitch results in zero "roll" by definition. However, it also requires an axis about which the pitching motion is given by a single rotation. This axis is termed the pitch axis and has a direction given by $\mathbf{a}_P = \mathbf{n}_D \times \mathbf{j}$. It lies in the x - z plane and makes an angle with the positive z -axis denoted as η , the "pitch direction". It is the angle in the x - z plane that the projection of the deck normal points. Note that the horizontal normal to the pitch axis makes an angle η with respect to the positive x -axis, and either can be used to determine the value of η .

A yaw angle can be defined by first rotating the platform about the pitch axis so that deck normal is vertical (i.e. the deck is horizontal). The change in direction of one of the platform column normals can then be used to define the yaw. This is written mathematically by defining a rotation matrix about the y -axis by η as $\mathbf{R}_y(\eta)$, and about the z -axis by the pitch angle as $\mathbf{R}_z(\theta_p)$. Rotating the platform to vertical is given by the rotation matrix $\mathbf{R}_V = \mathbf{R}_y(-\eta) \mathbf{R}_z(\theta_p) \mathbf{R}_y(\eta)$. Application of \mathbf{R}_V to either of the platform column surface normals (\mathbf{n}_{Cx} or \mathbf{n}_{Cz}) allows a yaw angle to be defined as the angle between the initial orientation of the x -column normal \mathbf{n}_{Cx} and $\mathbf{R}_V \mathbf{n}_{Cx}$ (or equivalently between the initial orientation of the z -column normal \mathbf{n}_{Cz} and $\mathbf{R}_V \mathbf{n}_{Cz}$).

PLATFORM KINEMATICS

The pitch response of the platform for each mooring system is shown in **Figure 5** as a function of wave impact angle. For each platform, the maximum pitch occurs at approximately 10 s and is predicted to be insensitive to wave impact angle except for the 8-LS system in which there is a small reduction in pitch with increasing wave angle. Maximum pitch is approximately 8.5° for the 8-LS system, 8.75° for the 8-LPS, 9° for the TLP and 10° for the TSM. Although maximum pitch is not strongly dependent on wave impact angle, the pitch history has a significant dependence on it.

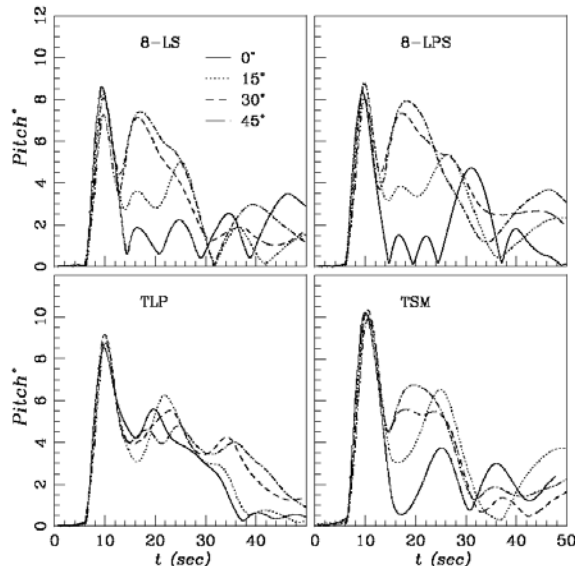


Figure 5: Pitch response for different wave impact angles for the 4 different mooring systems.

For normal (0°) impact (solid lines in Figure 5) the pitch for platforms with diagonal cables (8-LS, 8-LPS, TSM) returns to close to zero at around 14-16 s, although each experiences subsequent oscillations in pitch of varying magnitudes. These oscillations correspond to changes in the pitch direction (η) from approximately 0° to 180° (i.e. from pointing in the positive x-direction to the negative). For these same three mooring systems, as the impact angle increases, the return to horizontal is slower with a second large peak around 5-6° observed for 30 and 45° wave impacts (once again the pitch direction changes to the negative x-axis for these second peaks).

The TLP pitch behaviour is different with a much slower return toward horizontal at around 40 s without the oscillatory behaviour of the other mooring systems. These differences are illustrated in Figure 6 which shows a sequence of images at 8, 10, 12 and 16 s for the 8-LS and TLP systems during a normal wave impact. The maximum pitch, surge and heave for the 8-LS occur at 10, 12 and 15 s respectively and for the TLP at 10, 30 and 15 s.

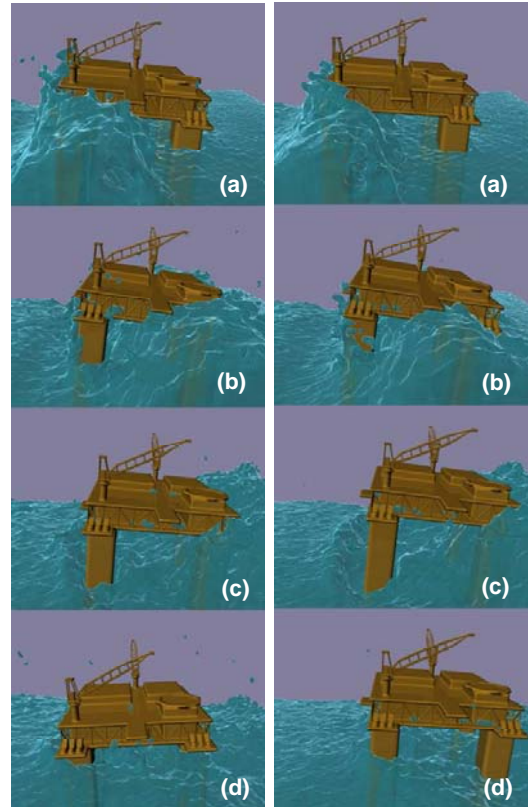


Figure 6: Side view of 8-LS (left) and TLP (right) platforms for normal (0°) wave impact. From top to bottom times are 8, 10, 12 and 16 s.

The more rapid return towards horizontal for the platforms with diagonal cables can be explained by considering the wave impact sequence in more detail. As the wave impacts, the initial response is a pitch motion driven by a large force on the top of the platform (as seen in Figure 6a, e). This is followed by a surge motion in the direction of the wave impact as seen in Figure 6 and quantified in Figure 7. The surge is predicted to be insensitive to impact angle although it is strongly dependant on the mooring system.

The surge responses of the 8-LS and TSM systems are almost indistinguishable with a peak of approximately 20-22 m at 12 s. There is a rapid recovery in surge for both platforms and they return and overshoot their initial position around 32-36 s. The 8-LPS system is similar although the peak surge is greater at 26 m and occurs slightly later at 14 s and the 8-LPS does not recover fully until after 50 s. The general form of the surge response for mooring systems with diagonal cables is however similar. The outlier is the TLP which records a maximum surge at around 30 s and which only very slowly returns. Again, this is due to a lack of restoring force in the wave direction due to the vertical TLP cables.

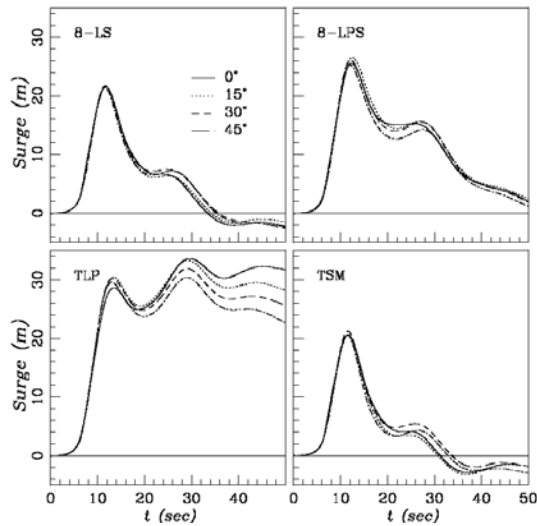


Figure 7: Surge response for the different mooring systems at 4 different wave impact angles.

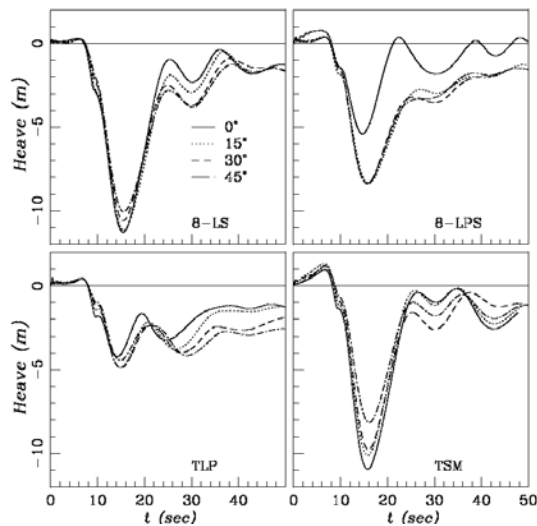


Figure 8: Heave response for different mooring systems at 4 different wave impact angles.

The surge motion increases tension in the impact-side cables and for angled cables, produces a large downward force on the impact-side column (or columns). This downward force induces a heave motion in the platform as well as creating torque of an opposite sense to the one resulting from initial wave impact.

Figure 8 shows the heave response. The peak heave lags the peak surge by 2-4 s and not a strong function of wave angle. The 8-LS and TSM heave responses are very similar at about -11 m. The 8-LPS has a similar form albeit with a smaller surge (-8 m) and the TLP surge is just -5 m. The larger heave motion for diagonal cables is discussed in Rudman *et al.* (2008) and is primarily an effect of mooring geometry.

Returning to the discussion of pitch response, once the wave has passed the leading column(s) (Figure 6b) they enter the trough following the wave. Thus buoyancy is lost on this side of the platform at the same time as the wave crest passes the non-impact side columns increasing the buoyancy there. This buoyancy distribution leads to a strong restoring torque in all cases. The mechanism is similar for all wave impact angles as shown in Figure 9

for a 45° wave impact on the 8-LS and TLP mooring systems. However the additional restoring torque induced from cable tensions in the diagonal cables is negligible in the TLP with only vertical cables, and the pitch return is consequently much slower for the TLP.

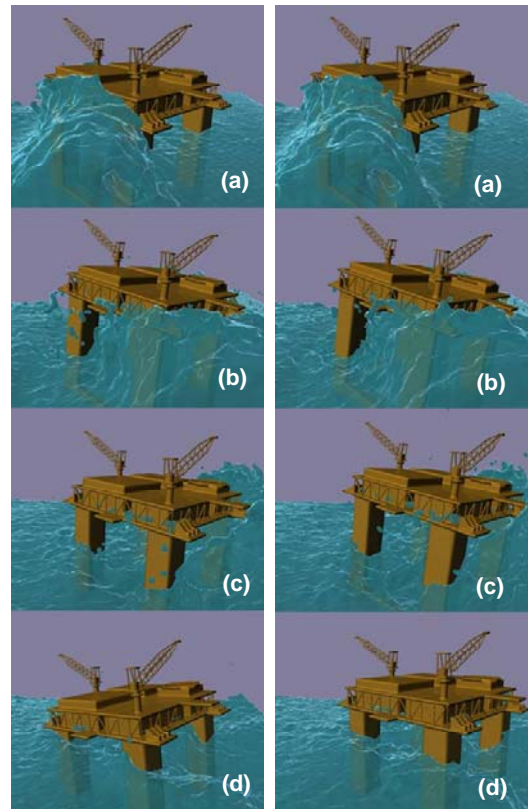


Figure 9: Side view of 8-LS (left) and TLP (right) platforms for a 45° wave impact. From top to bottom times are 8, 10, 12 and 16 s.

The yaw response of the platforms (not shown) is fairly small and less than 4° for 0° and 45° impacts although as high as about 12° for 15° and 30° impacts. This is unsurprising given the non-symmetric wave forces for angles other than 0 and 45°. Similarly, the sway (z -axis) response is small (not shown), being less than 2.5 m.

In summary, as a result of the wave impact, all platforms experience significant pitch, the maximum for each being almost independent of wave impact angle. The 8-L systems perform a little better with the TSM performing the worst. Surge and heave response are broadly insensitive to wave angle, but vary between mooring systems. All systems undergo significant surge with the TLP giving the highest followed by the 8-LPS mooring system. All systems with diagonal cables undergo significant heave, however the polyester cables of the 8-LPS system allow more stretch than the steel cables of the 8-LS and TSM systems, so the heave is less than for the other diagonal systems. The 8-LPS system has some of the advantages of the TLP system with a reduced heave, and some of the advantages of the TSM system with reduced surge and has the second lowest maximum pitch.

MOORING LINE TENSION

The mooring line tension is always the highest in the leading column cable (cable 1 in Figure 3) or the two

leading cables for 0° wave impacts (cables 1 and 2). This maximum tension is shown in separate plots for vertical and diagonal cables in Figure 10. (Note that the TSM has no vertical cables and the TLP has no diagonal ones, hence their absence from the vertical and diagonal plot respectively.) The trend for both cable types is that as the impact angle increases the cable tension increases significantly and (not shown) the tension in cable 2 decreases significantly. Thus the leading cable in the 45° wave impact case is always the worst-case design scenario.

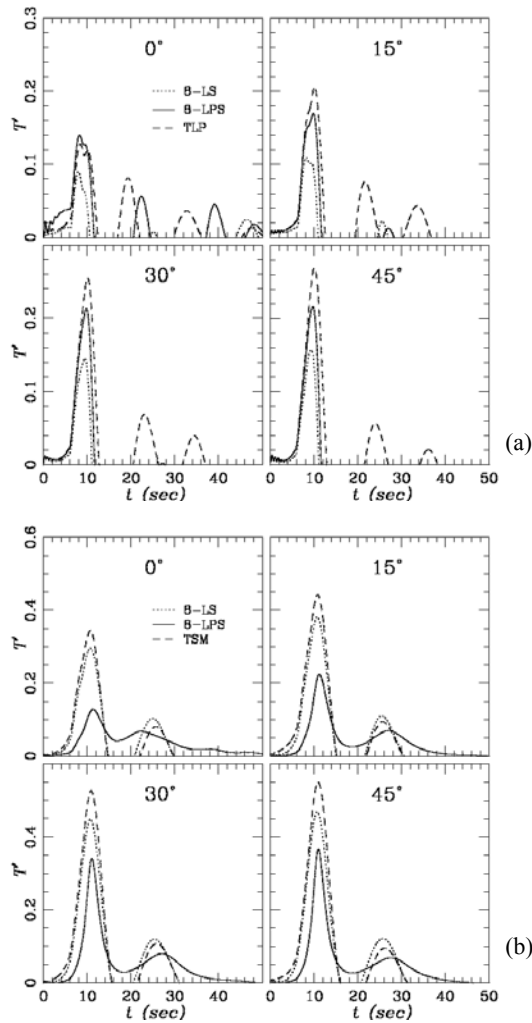


Figure 10: Cable tension in leading edge (a) vertical mooring cables and (b) diagonal cables. Tension has been normalised by the platform weight.

Figure 10 also shows that in the 8-L systems the tension in the diagonal cables is always higher than in the vertical ones. (It is also the case when comparing the TLP to TSM.) The ratio of tensions in diagonal to vertical cables (and in TSM tension to TLP tension) is reasonably insensitive to wave impact angle with the ratio of tensions being approximately 3 for the 8-LS system, 2.0 for the TLP vs. TSM and 1.6 in the 8-LPS system. This result suggests that to more evenly distribute the forces in the cables, especially in the 8-LS case, higher initial tension in the vertical cables is potentially desirable. The maximum tensions in an 8-L system is always less than the tension in the equivalent cable in the TLP or TSM

system. This is expected since the 8-L systems have twice the number of cables to distribute the force over.

Of most interest in the tension results is the reduced tension in the diagonal polyester cables of the 8-LPS system and the more closely balanced tension between vertical and diagonal cables (a factor of 1.6 different) for this configuration. The tension rises more slowly in the polyester diagonal cables than for equivalent steel cables, and also fall more slowly. Since the polyester cables provide lower restoring force and torque for a given surge, the platform is able to move further in the wave direction (higher surge) and the vertical steel cables begin to take more of the load. This lessens the total tension apportioned to the diagonal cables. In contrast to steel diagonal cables, in most cases tension in the polyester cables does not fall to zero as the tension decreases. This is a potentially beneficial safety feature. The release and sudden reapplication of tension when the platform is moving with speed can impart dangerous forces on the moorings and is ideally to be avoided.

CONCLUSION

The TLP and TSM mooring systems have previously been shown to have significantly different responses to rogue wave impact. Combining both mooring systems with the same steel cables, (i.e. 8-LS) results in behaviour that is very similar to the TSM system. Although there is a small reduction in maximum pitch, the surge and heave response is almost identical. In terms of cable tension, the 8-LS system has approximately 20% lower tension than the TSM in the diagonal cables and about 30% lower than the TLP in the vertical cables. With the low amount of weight supported in the vertical tensioned cables, this system offers very little advantage over the simpler TSM. Further work is required to investigate how increased tension in these cables might modify this situation. When the steel diagonal cables are replaced by polyester ones (the 8-LPS system), the platform motion changes more. The maximum pitch is marginally better than the TLP however the surge and heave response is part way between TLP and TSM, with lower surge than the TLP and larger heave than the TSM. The 8-LPS system also has lower overall tension in the diagonal cables and a more uniform partition of tension between vertical and diagonal cables. This partitioning could perhaps be further improved by changing the initial tension in the vertical steel cables.

The effect of wave impact angle is not significant for most of the platform motions. The exception is the yaw response for 15 and 30° impacts is larger. The primary effect of impact angle is to increase the tension in the leading cable as the angle changes from 0 to 45° . Hence 45° impacts are the ones that must be designed for in practice.

These mooring configurations are just a few of the different ones that can be used in practice, and a rational process is required to determine the advantages and disadvantage of each in extreme event scenarios such as rogue wave impact. The use of the SPH as illustrated in this paper is seen to be an excellent choice to model this complex non-linear fluid-structure interaction.

REFERENCES

- BUNNICK, T. and BUCHNER, B. 'Numerical predictions of wave loads on structures in the splash zone', *Proceedings of the 14th International Polar and Offshore Engineering Conference*, Toulon France 23-28 May 2004.
- CLEARY, P. W., 'Modelling confined multi-material heat and mass flows using SPH', *Appl. Math. Modelling*, **22**, 981-993, (1998).
- CLEARY, P.W., and PRAKASH, M., 'Smooth Particle Hydrodynamics and Discrete Element Modelling: potential in the environmental sciences', *Philosophical Transactions A*, **362**, 2003-2030, (2004).
- CLEARY, P.W. and RUDMAN, M. 'Extreme wave interaction with a floating oil rig', *Accepted for publication in Progress in CFD* 2009.
- FALTINSEN, O.M., 'Wave loads on offshore structures', *Ann. Rev. Fluid Mech.* **22** 35-56 (1990).
- GOMEZ-GESTEIRA, M., CERQUEIRO, D., CRESPO, C. and DALRYMPLE, R.A. 'Green water overtopping analyzed with a SPH model', *Ocean Eng.* **32** 223-238 (2005).
- JAIN, A.K., 'Non-linear coupled response of offshore tension leg platforms to regular wave forces', *Ocean Eng.* **24** 577-592 (1997).
- KLEEFMAN, K.M.T., FEKKEN, G., VELDMAN, A.E.P., IWANOWSKI, B. and BUCHNER, B. 'A volume-of-fluid based simulation method for wave impact problems', *J. Comput Phys.* **206** 363-393 (2005).
- MONAGHAN, J.J. 'Smoothed Particle Hydrodynamics', *Ann. Rev. Astron. Astrophys.* **30** 543-574 (1992).
- MONAGHAN, J.J. 'Simulating free surface flows with SPH', *J. Comput. Phys.* **110L** 399-406 (1994).
- NIELSEN, F.G., 'Comparative study on air-gap under floating platforms and run-up along platform columns', *Marine Structures* **16** 97-134 (2003).
- PETRUSKA, D, GEYER, J., MACON, R., CRAIG, M. RAN, A. and SCHULZ, N., "Polyester mooring for the Mad Dog spar – design issues and other considerations", *Ocean Eng.*, **32** 767-782 (2005).
- RAOOF, M. and KRAINCANIC, I., 'Analysis of large diameter steel ropes', *J. Eng. Mech.* **121** 667-675 (1995).
- RUDMAN, M., CLEARY, P.W., SINNOTT, M.D. and SYLVESTER, T., "Computational Modelling Of Free Surface Flows For Offshore Application", *Marine Sys. & Ocean Tech.* **3** 113-122, (2007).
- RUDMAN, M., CLEARY, P.W., LEONTINI, J., SINNOTT, M.D. and PRAKASH, M., "Rogue wave impact on a semi-submersible offshore platform", *OMAE2008, 27th Int. Conference on Offshore Mechanics and Arctic Engineering* 15th-19th June 2008, Estoril Portugal
- RUDMAN, M. and CLEARY, P.W., 'Oblique Impact of Rogue Waves on a Floating Platform', *Proc. 19th Int. Offshore and Polar Eng. Conf.*, Osaka, Japan, June, (2009)
- SHAO, S. 'Incompressible SPH simulation of wave breaking and overtopping with turbulence modelling', *Int. J. Numer. Meth. Fluids* **50** 597-621 (2006).